Volume 11, Issue 1
February 2022

ITEE Journal

ISSN: - 2306-708X

Automatic Segmentation of Breast Tumors in Mammograms using Fuzzy Clustering

[1]Sarbjit Kaur, [2]Jasmeen Gill and [3]Gagandeep Jagdev

[1]Department of Computer Science & Engineering, School of Engineering, RIMT University, Mandi Gobindgarh, Punjab, India

[2]Department of Computer Science & Engineering, School of Engineering, RIMT University, Mandi Gobindgarh, Punjab, India

[3]Department of Computer Science, Punjabi University Guru Kashi Campus, Damdama Sahib, Punjab, India

Email: [1]sabby13dhillon@gmail.com, [2]er.jasmeengill@gmail.com, [3*]drgagan137@pbi.ac.in

ABSTRACT

Image segmentation is the process via which the digital image understudy is partitioned into multiple segments. The purpose of the segmentation is to convert the representation of the image into something more significant and easier to examine. The primary aim of image segmentation in mammography is to find the hazardous objects (lesions, dense breast tissues, and microcalcifications) and boundaries of the mammograms. Segmentation assigns a label to each pixel in an image in such a manner that the pixels with the same label share certain characteristics. The research paper elaborates a proposed method for performing segmentation of the mammograms. The mammogram images from the DRIVE database have been used to conduct the research work. The proposed model is detailed via a flowchart followed by an elaborated algorithm specifying the adopted process for conducting the segmentation. The values of 16 performance evaluation parameters for 16 different mammograms have been obtained to prove the worthiness of the conducted research. The GUI has been designed to perform the implementation easily and contentedly.

Keywords: *Breast cancer, CLAHE, Mammograms, Morphological operations, Region of Interest, Segmentation.*

1. INTRODUCTION

In the last two decades, image processing has played a crucial role in examining and solving the issues in medical imaging. The researchers anticipated diverse segmentation procedures but still did not recommend a mutual method that can be appropriate to all types of applications [1, 2]. The image is divided into multiple segments based on properties like color, brightness, reactivity, and texture. Segmentation recognizes the ROI (Region of Interest) in automating or supporting the description of anatomic structures [3]. Segmentation helps in the detection of microcalcifications, masses, and hazardous lesions [4, 5]. The research paper elaborates the proposed model for conducting segmentation of mammograms for timely diagnosing breast cancer in women. The conducted research makes use of certain performance evaluation parameters out of which the prominent evaluation parameters are briefly defined below.

- True positive (TP) – True positive is defined as the patient having the disease and being identified as having the disease.
- False-positive (FP) – False-positive is defined as the patient not having the disease and identified as having the disease.
- True negative (TN) – True negative is defined as the patient not having the disease and identified as not having the disease.
- False-negative (FN) – False-negative refers to the patient having the disease and identified as not having the disease.
- Sensitivity (True-Positive Rate) - The true positive rate (TPR) is the proportion of the individual with a known positive condition for which the test result is positive [6, 7]. This rate is often known as Sensitivity.

  TPR (Sensitivity) = TP / (TP + FN)
- Specificity (True-Negative Rate) - The true negative rate (TNR) is the proportion of the individuals with a known condition for which the test result is negative [8, 9]. This rate is often called Specificity.

  TNR (Specificity) = TN / (TN + FP)
- False-Positive Rate (FPR) - The false-positive rate is the proportion of the individuals with the known negative condition for which the test result is positive.

  FPR = FP / (FP + TN)
- False-Negative Rate (FNR) - The false-negative rate is the proportion of the individuals with a known positive condition for which the result is negative. This rate is sometimes called the miss rate.

  FNR = FN / (TP + FN)
- False discovery rate (FDR) - FDR refers to the proportion of the number of FP results to the sum of FP and TP test results.

  FDR = FP / (FP + TP)
- False omission rate (FOR) – FOR refers to the ratio of the number of FN results to the number of total negative test results.

  FOR = FN / (TN + FN)
- Accuracy – Accuracy is the measure of closeness of a measured value to an acknowledged value [10, 11].

  Accuracy = (TP + TN) / (TP + TN + FP + FN)

- Matthews correlation coefficient (MCC) – The correlation coefficient between the observed and predicted binary values is referred to as MCC and possesses a value between −1 and +1.

  MCC = (TP*TN - FP*FN) / sqrt ((TP + FP) (TP + FN) (TN + FP) (TN + FN))

- F1 Score - The F-score, also called the F1-score, is a measure of a model's accuracy on a dataset. The F-score is a way of combining the precision and recall of the model, and it is defined as the harmonic mean of the model's precision and recall [12].

  F1 Score = TP / (TP + 0.5* (FP + FN))

- Markedness - Markedness quantifies how marked a condition is and specifies the probability that a condition is accurately marked. The value of markedness depends on the value of FPA (False positive accuracy) and FNA (False negative accuracy)

  Markedness = 1 – FPA - FNA

2. STATE OF ART

In 2021, Sarada Ghosh et al. [13] declared breast cancer as a dreadful disease among women which causes a serious impact on health and may cause a threat to life. Mammography is presently the best way to diagnose breast cancer. The authors made use of mammogram images with 1024 * 1024 pixels. Different approaches on classification have been analyzed and the authors declared that SVM (Support Vector Machine) performs better in terms of classification accuracy rate as compared to other prominent models. The authors extended their research work to FCM (Fuzzy C-Means), multi-model ensembles method, SVM combination method, and FCM clustering-based SVM model. The segmentation performed using the FCM clustering method enables a single piece of data to fit into multiple clusters. The conducted simulation offers the accuracy of 91.39% and 0.964 area under the ROC curve for mini-MIAS which proved the worth of the conducted research. In 2020, Nasibeh Saffari et al. [14] stated that because of low contrast and substantial variations in the mammograms, the evaluation of breast density with visual evaluation is still a challenging task. To perform the accurate classification of mammograms, it is necessary to detect the dense tissues in the mammographic images precisely. Several methods have been proposed to perform breast density estimation but they are not fully automated. Rather, these are adversely exaggerated by a lower signal-to-noise ratio and by the inconsistency of density in texture and appearance. The authors focused on developing a fully automated and digitized breast tissue segmentation and classification using advanced deep learning techniques. The cGAN (conditional Generative Adversarial Networks) have been applied to get the dense tissues segmented in mammograms. The authors proposed a CNN (Convolutional Nural Network) to classify mammograms as per BI-RADS (Breast Imaging-Reporting and Data System). The authors used 410 images of 115 patients from the INbreast dataset for performing the mammography. In 2019, Alam et al. [15] proposed a machine learning approach for the detection of benign and malignant microcalcification (MC) clusters. So the microcalcification classification technique is applied to segment digital mammogram images. Segmentation with the wavelet-based method and morphological operations is used to identify the size and the total number of calcification in an MC cluster. ROI (Region of Interest) is enhanced after the MC cluster is classified using a stack-generalization-based classifier. The authors made use of DDSM (Digital Database for Screening Mammography), MIAS (Mammographic Image Analysis Society), and achieved an accuracy of 96 percent. In 2019, Kamil et al. [16] stated that breast cancer is a very dangerous disease in women. It is diagnosed by using various techniques like sonar and mammography, but the limitation of these techniques is it contains noise, weak illumination, and an overlapping region. Segmentation is the method to reduce these limitations. So fuzzy morphological operations are used for segmentation. Fuzzy morphological operations are compared with the classical morphological operation with the help of a mini-MAIS database and results indicate that fuzzy morphological operations have achieved high accuracy. In 2018, A. Arokiyamary Delphia et al. [17] stated that breast cancer has been a major cause responsible for the maximum number of deaths related to cancer among women. It is really difficult to detect cancer-relevant tumors at an early stage which makes the cure furthermore complicated and intense. Manually dealing with such cases is time-consuming and inefficient. So the need arises for developing and coming up with such methods that are efficient in diagnosing the cancerous cells without any human intervention and that too with perfectness. Mammography is one such special case of CT scan which adopts the X-ray technique and utilized high-resolution film to detect the tumors with perfection in the breast. The research paper described different image processing techniques. Different conventional tactics related to image processing were discussed in the paper. The method defined in the research paper comprises all the segmentation detection algorithms for both single view and multi-view mammograms and proved that how these techniques are suitable for breast region segmentation and ROI segmentation. In 2018, Dinesh Pandeya et al. [18] stated that during the analysis of breast-relevant magnetic resonance images, the main challenge is to perform precise segmentation of ROI (region of interest) and BD (breast density). Several existing methods for performing segmentation of mammograms can be classified as semi-automatic and limited on the scale of perfection. The cause behind this is the difficulty faced in the removal of landmarks from noisy MRI (Magnetic Resonance Images) having the same intensity levels. The paper also illustrated that precise and outstanding results were displayed by pixel-based quantitative analysis when manually compared with BD and BROI. The authors obtained results of performance metrics like specificity, accuracy, an area under the curve, etc. which proves the worth of research conducted. The average computational time was calculated to 1 minute 50 seconds for performing the segmentation. In 2016, K.D. Marcomini et al. [19] stated that Ultrasonography is the best technique for screening mammograms. In this paper, various techniques (median filter, thresholding, clustering) are used to check the lesions

in ultrasonography and the classification of benign and malignant breast tumors. Firstly mammogram images are taken from the breast phantoms and laboratories, which pre-process the mammogram image and find the region of interest using wiener filtering and median filter. Segmentation with the help of fuzzy-c means clustering and classification with the help of multilayer perceptrons (MLP) and achieves an accuracy of 94 percent.

3. RESEARCH METHODOLOGY

This section elaborates the research methodology adopted for performing the segmentation of the mammograms. Fig. 1 shows the flowchart of the proposed model to perform segmentation of the mammograms.

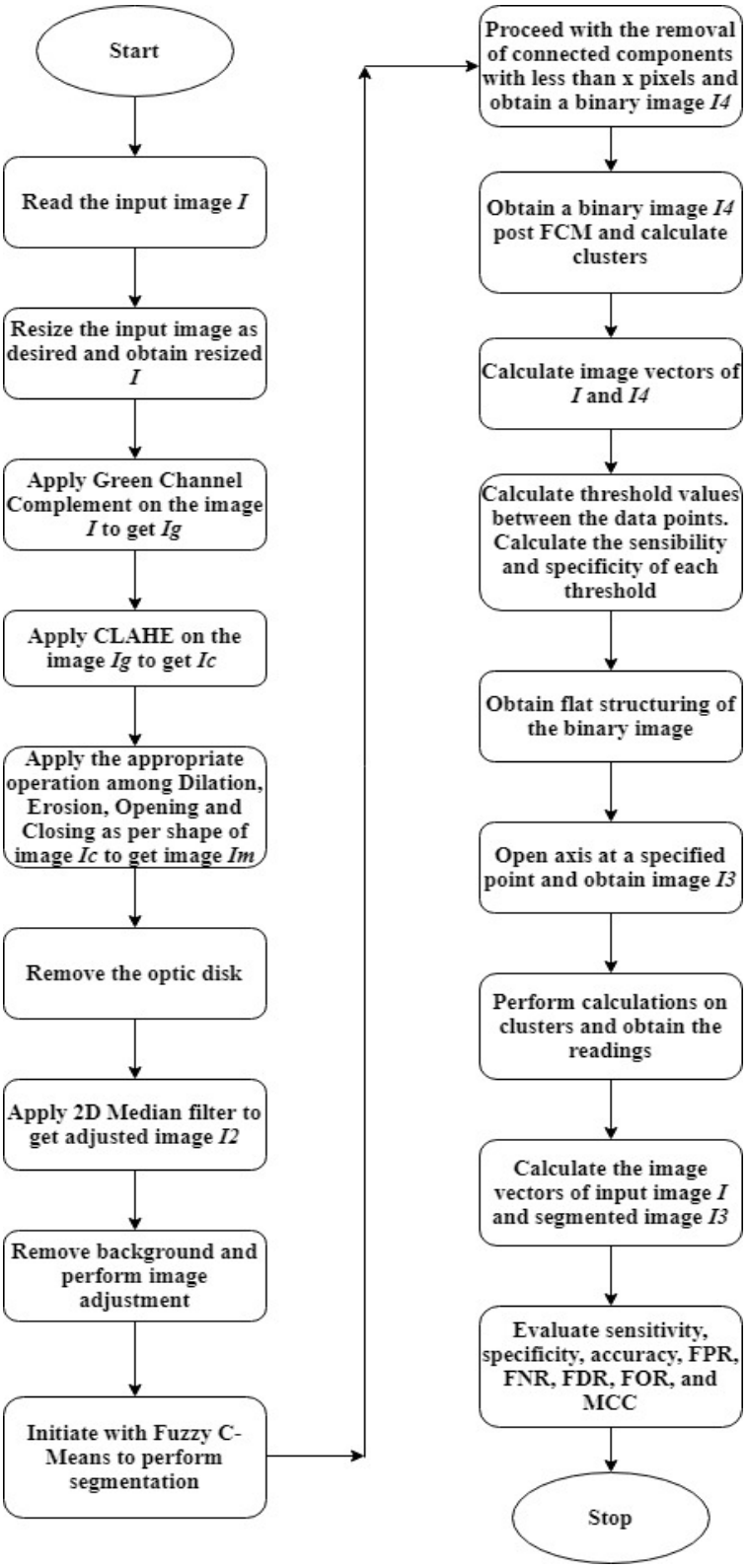

Fig. 1. Flowchart of the proposed method for performing segmentation of mammograms

4. IMPLEMENTATION AND RESULTS

This section depicts the practical implementation of the proposed methodology elaborated in Section III. The mammogram images from MIAS (Mammographic Image Analysis Society) database have been used as input. The implementation has been performed on three mammogram images from the MIAS database and the step-wise process is depicted in the three instances mentioned below.

Instance 1

Input Mammogram Image - Mdb010.pgm

Fig. 2(a) depicts the input mammogram image *I (Mdb010.pgm)* from the MIAS benchmark database. The input image *I* undergo Green Channel Complement to produce image *Ig* as shown in Fig. 2(b). The image *Ig* is provided as input to CLAHE and the contrast limited image *Ic* is obtained as depicted in Fig. 2(c). The shape of the image *Ic* is used to determine the appropriate morphological function intended to remove the imperfections accounting for the form and structure of the image under study shown in Fig. 2(d). Thereafter, the segmentation of the image *I4* is conducted as shown in Fig. 2(e). The value of the two clusters is obtained and finally, the segmented edge detection is performed as shown in Fig. 2(f).

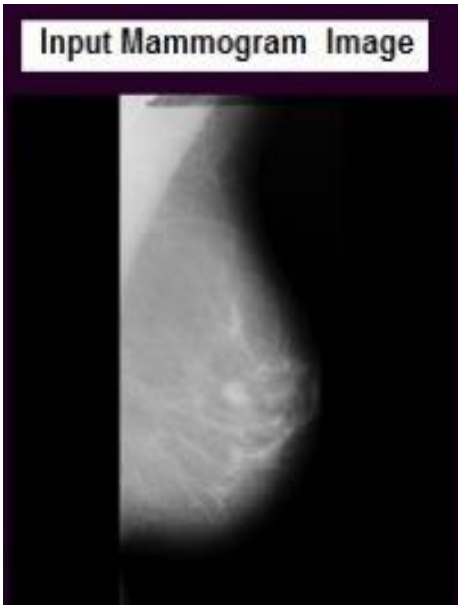

Fig. 2(a). Input Mammogram image *I*

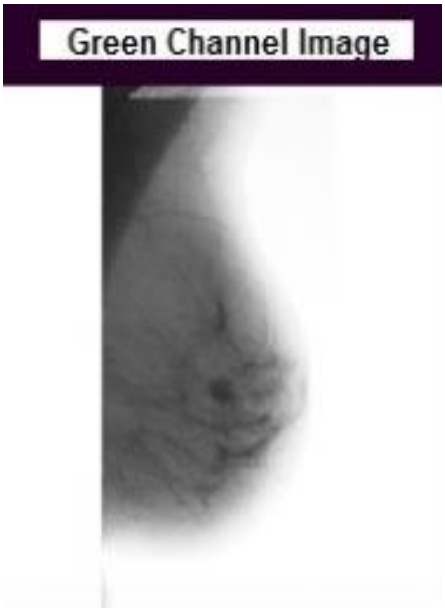

Fig. 2(b). Green Channel Image *Ig*

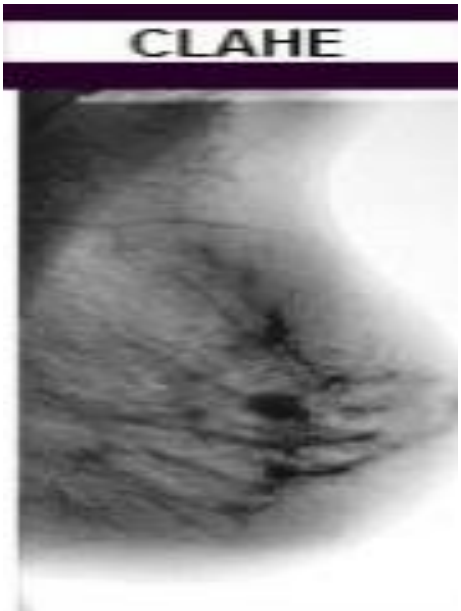

Fig. 2(c). Image *Ic* obtained post-CLAHE

Fig. 2(d). Image obtained from Morphological operations

Fig. 2(e). Segmented Image *I4*

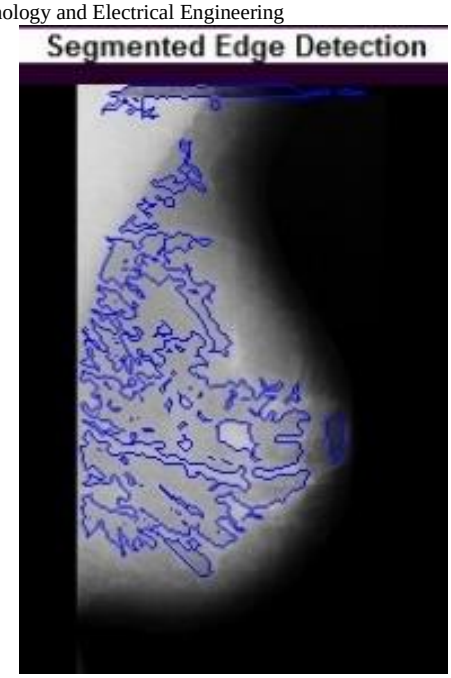

Fig. 2(f). Segmented Edge Detection

Fig. 3 shows the GUI constructed to display the different stages through which the input image proceeds for segmentation.

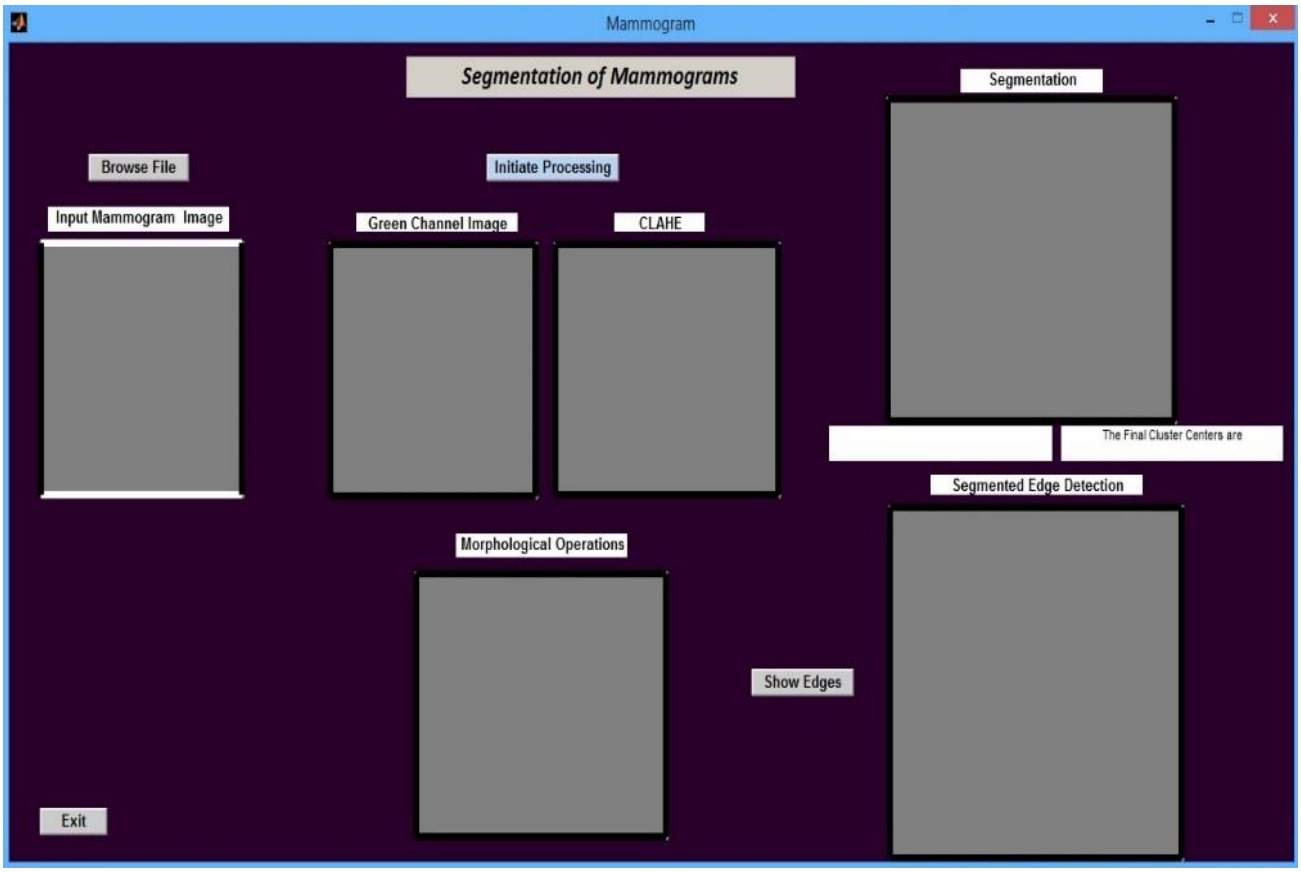

Fig. 3. Designed GUI as per the proposed method to perform segmentation

Fig. 4 shows the image *Mdb010.pgm* been uploaded as the input image and the images obtained from Green Channel Complement, CLAHE, Morphological Operations, and Segmentation displayed on the constructed GUI.

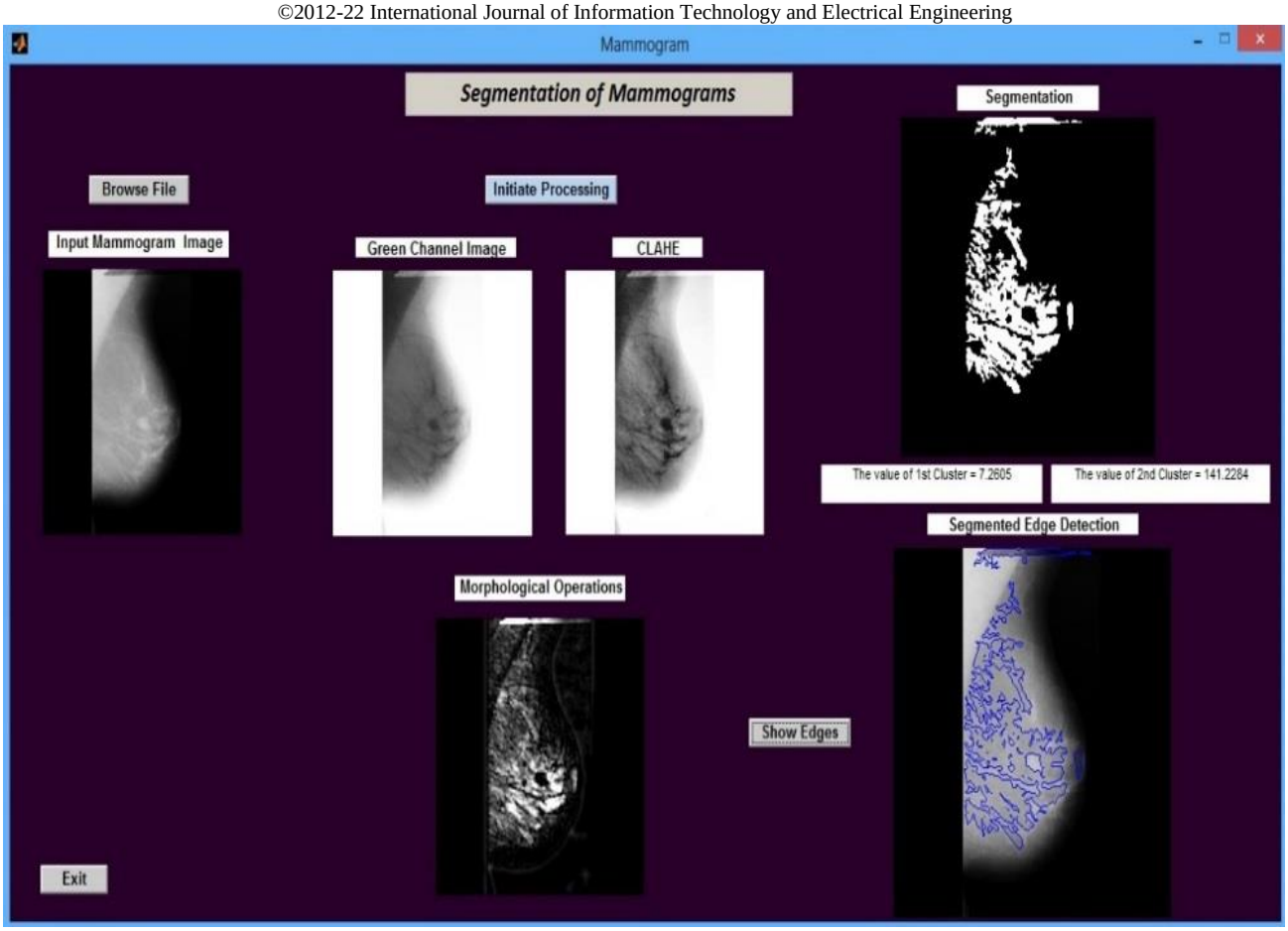

Fig. 4. GUI showing the different steps of segmentation through which the input image *Mdb010.pgm* underwent

The reading of different performance evaluation parameters for the input image *Mdb010.pgm* is depicted in Table 1 below.

Table 1. Calculated Parameters between Original and Segmented Image

Sr. No.	Parameters	Calculated Values
1	Distance	0.9334
2	Threshold	218
3	Sensitivity	0.0666
4	Specificity	0.9969
5	AROC	0.3537
6	Accuracy	0.9617
7	PPV	0.9554
8	NPV	0.5164
9	FNR	0.9334
10	FPR	0.0031
11	FDR	0.0446
12	FOR	0.4836
13	F1 Score	0.1245
14	MCC	0.1731
15	MK	0.4718

Instance 2:

Input Mammogram Image - Mdb011.pgm

Fig. 5(a) depicts the input mammogram image *I (Mdb011.pgm)* from the MIAS benchmark database. The input image *I* undergo Green Channel Complement to produce image *Ig* as shown in Fig. 5(b). The image *Ig* is provided as input to CLAHE and the contrast limited image *Ic* is obtained as depicted in Fig. 5(c). The shape of the image *Ic* is used to determine the appropriate morphological function intended to remove the imperfections accounting for the form and structure of the image under study shown in Fig. 5(d). Thereafter, the segmentation of the image *I4* is

conducted as shown in Fig. 5(e). The value of the two clusters is obtained and finally, the segmented edge detection is performed as shown in Fig. 5(f).

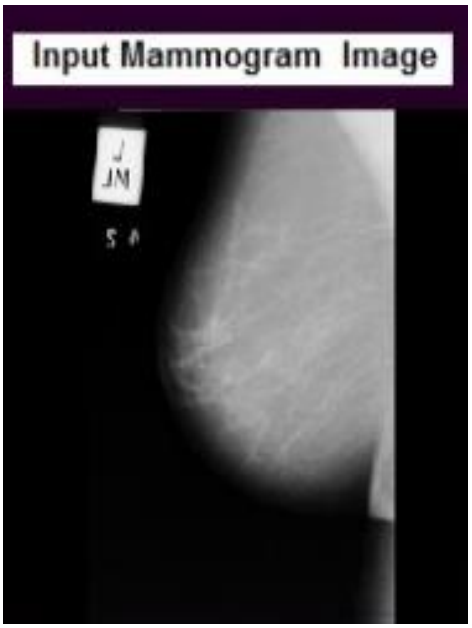

Fig. 5(a). Input Mammogram image *I*

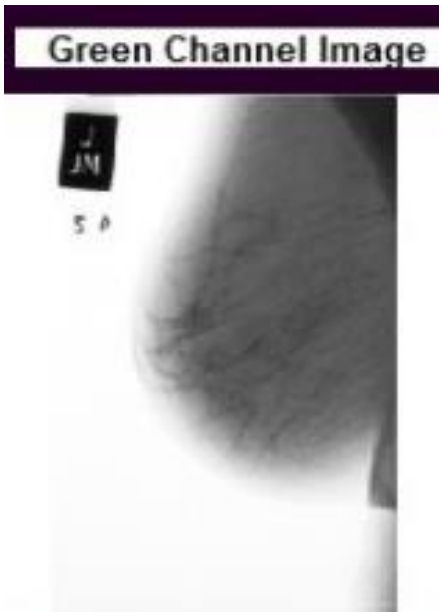

Fig. 5(b). Green Channel Image *Ig*

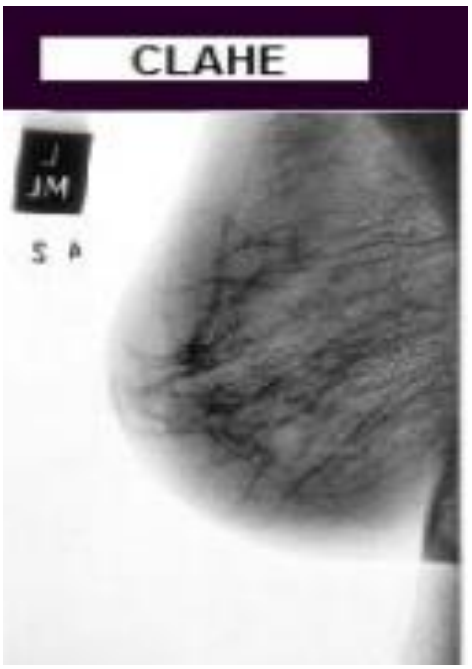

Fig. 5(c). Image *Ic* obtained post-CLAHE

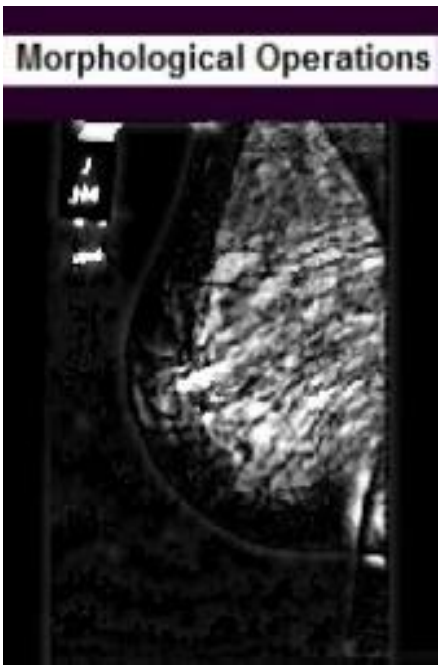

Fig. 5(d). Image obtained from Morphological operations

Fig. 5(e). Segmented Image *I4*

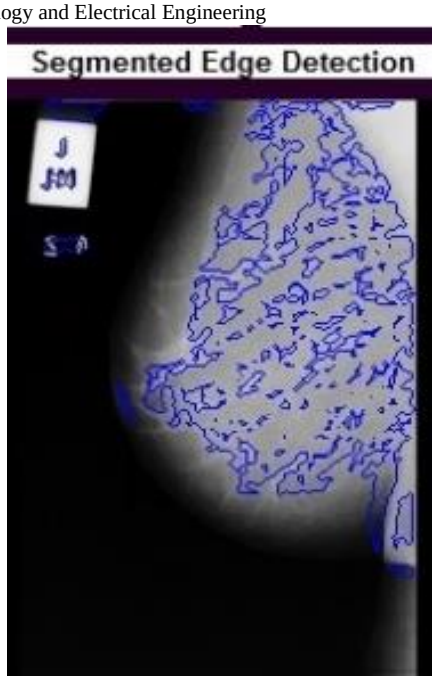

Fig. 5(f). Segmented Edge Detection

Fig. 6 shows the image *Mdb011.pgm* been uploaded as the input image and the images obtained from Green Channel Complement, CLAHE, Morphological Operations, and Segmentation displayed on the constructed GUI.

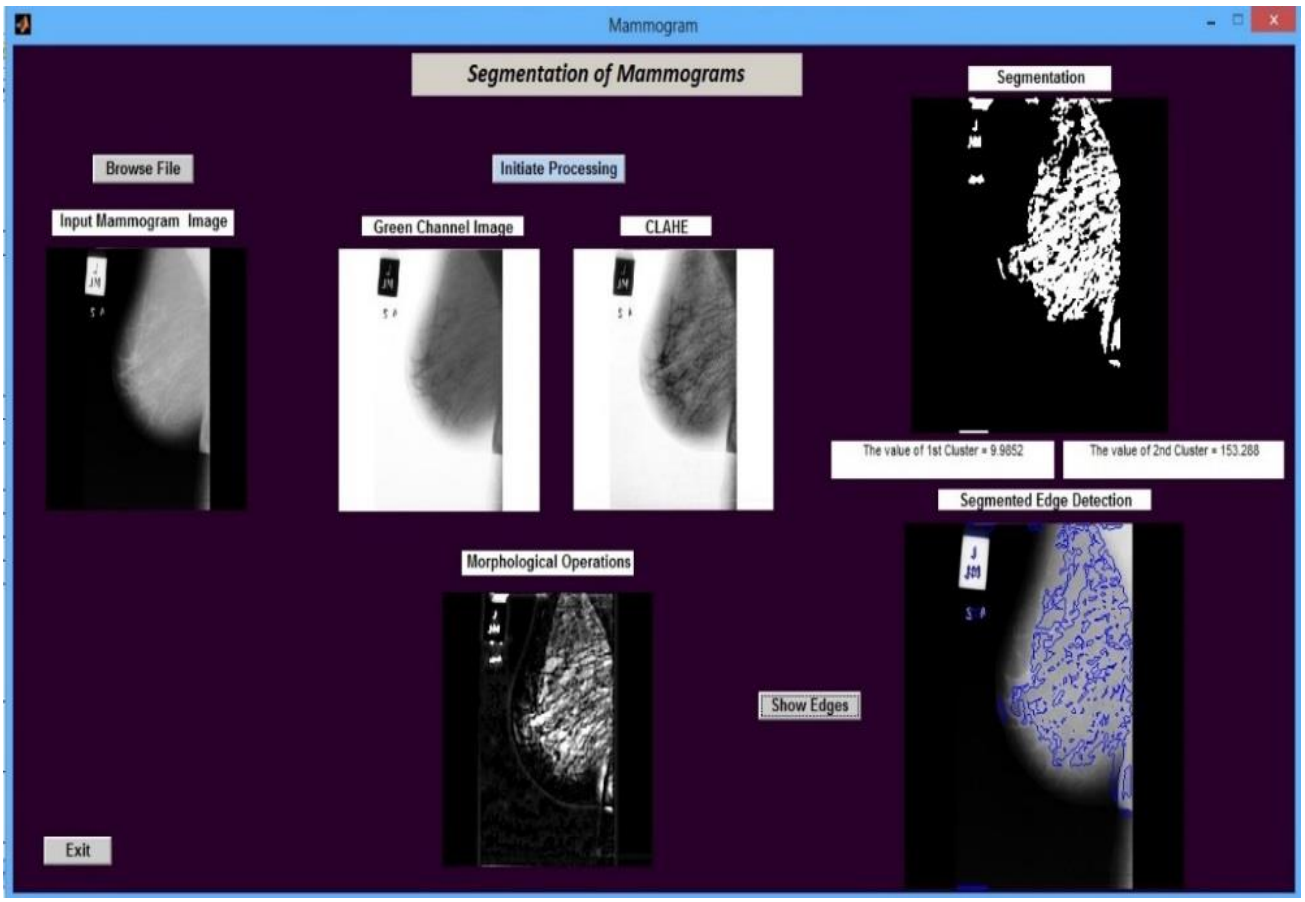

Fig. 6. GUI showing the different steps of segmentation through which the input image *Mdb011.pgm* underwent

The reading of different performance evaluation parameters for the input image *Mdb011.pgm* is shown below in Table 2.

Table 2. Calculated Parameters between Original and Segmented Image

Sr. No.	Parameters	Calculated Values
1	Distance	0.9335
2	Threshold	218.0000
3	Sensitivity	0.0666
4	Specificity	0.9846
5	AROC	0.2777
6	Accuracy	0.9556
7	PPV	0.8122
8	NPV	0.5133
9	FNR	0.9334
10	FPR	0.0154
11	FDR	0.1878
12	FOR	0.4867
13	F1 Score	0.1231
14	MCC	0.1291
15	MK	0.3255

Instance 3:

Input Mammogram Image - *Mdb012.pgm*

Fig. 7(a) depicts the input mammogram image *I (Mdb012.pgm)* from the MIAS benchmark database. The input image *I* undergo Green Channel Complement to produce image *Ig* as shown in Fig. 7(b). The image *Ig* is provided as input to CLAHE and the contrast limited image *Ic* is obtained as depicted in Fig. 7(c). The shape of the image *Ic* is used to determine the appropriate morphological function intended to remove the imperfections accounting for the form and structure of the image under study shown in Fig. 7(d). Thereafter, the segmentation of the image *I4* is conducted as shown in Fig. 7(e). The value of the two clusters is obtained and finally, the segmented edge detection is performed as shown in Fig. 7(f).

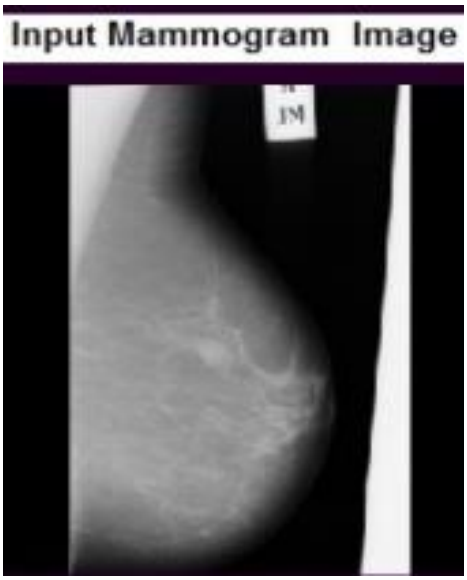

Fig. 7(a). Input Mammogram image *I*

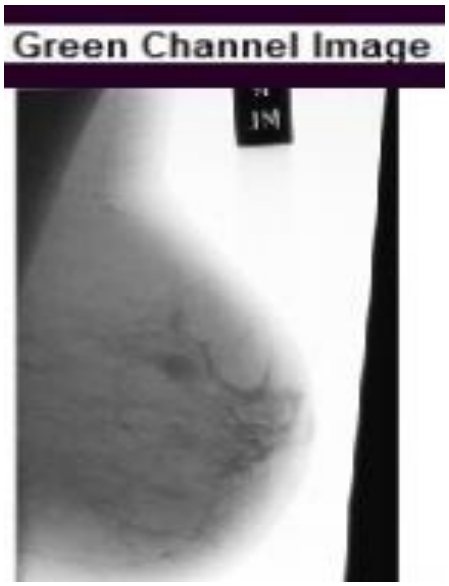

Fig. 7(b). Green Channel Image *Ig*

Fig. 7(c). Image *Ic* obtained post-CLAHE

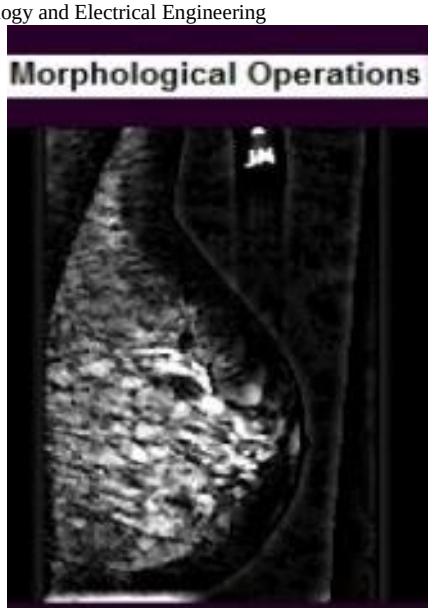

Fig. 7(d). Image obtained from Morphological operations

Fig. 7(e). Segmented Image *I4*

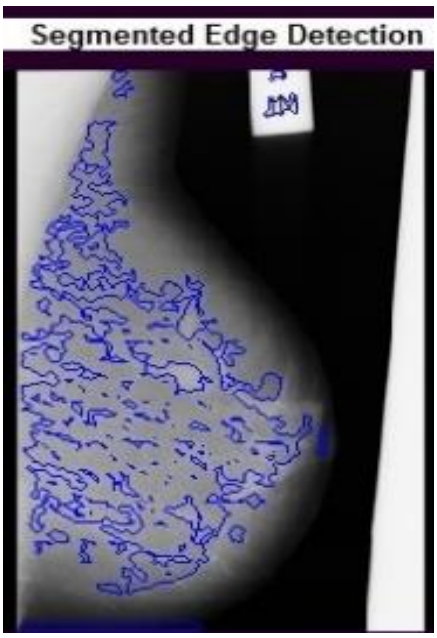

Fig. 7(f). Segmented Edge Detection

Fig. 8 shows the image *Mdb012.pgm* been uploaded as the input image and the images obtained from Green Channel Complement, CLAHE, Morphological Operations, and Segmentation displayed on the constructed GUI.

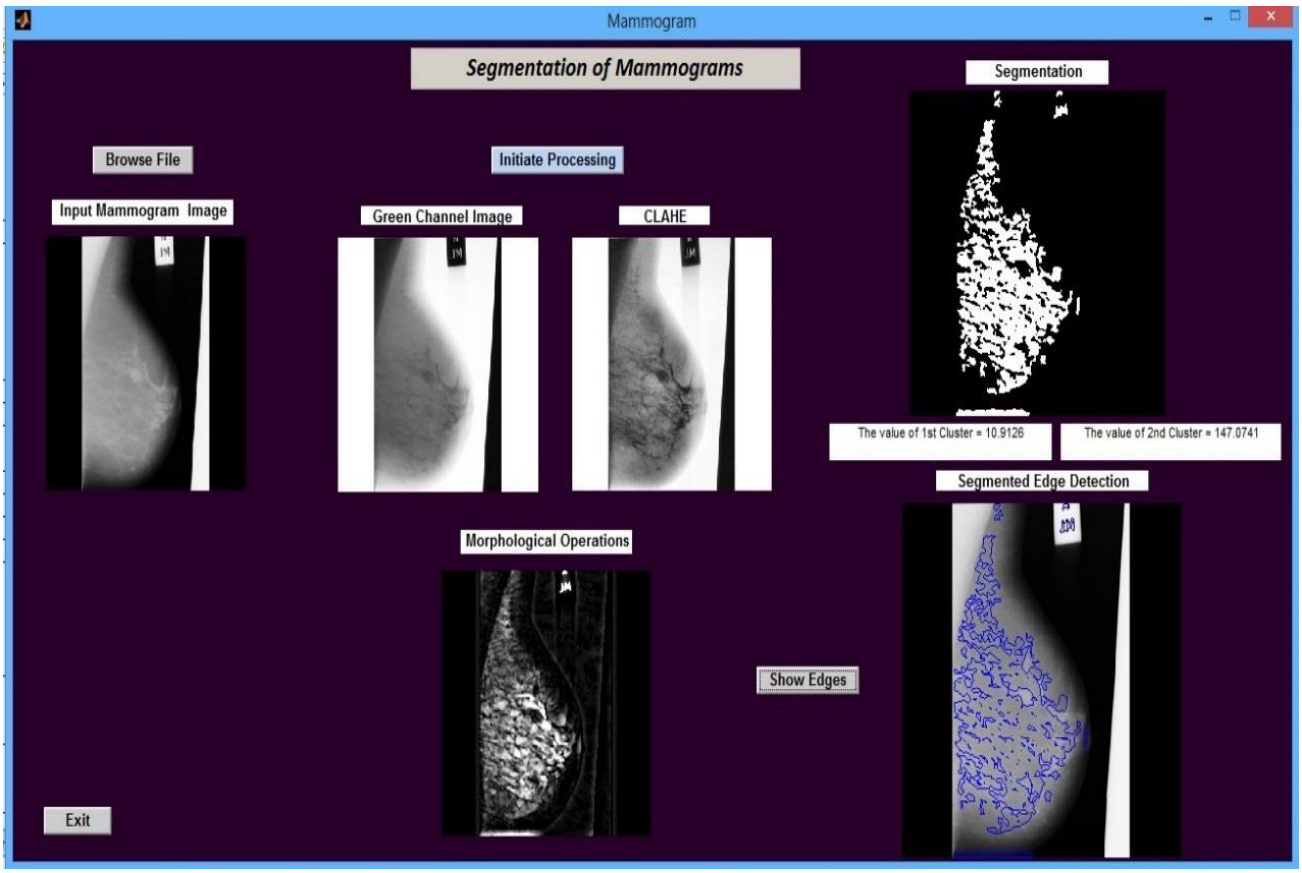

Fig. 8. GUI showing the different steps of segmentation through which the input image *Mdb012.pgm* underwent

The reading of different performance evaluation parameters for the input image *Mdb012.pgm* is shown below in Table 3.

Table 3. Calculated Parameters between Original and Segmented Image

Sr. No.	Parameters	Calculated Values
1	Distance	0.9356
2	Threshold	230.0000
3	Sensitivity	0.0663
4	Specificity	0.9414
5	AROC	0.2468
6	Accuracy	0.9338
7	PPV	0.5307
8	NPV	0.5020
9	FNR	0.9337
10	FPR	0.0586
11	FDR	0.4693
12	FOR	0.4980
13	F1 Score	0.1178
14	MCC	0.0159
15	MK	0.0328

5. RESULTS AND CONCLUSION

The 16 images from the MIAS database have been uploaded and segmented on the proposed model via constructed GUI. Table 4 shows the obtained readings of 16 attributes for 16 images from the MIAS database.

Table 4. Table shows the readings of different performance evaluation parameters for 16 mammograms analyzed from DRIVE database

Image (*.pgm)	009	010	011	012	013	014	015	100	101	102	103	104	105	106	107	108
Distance	.9338	.9334	.9335	.9356	.9334	.9335	.9334	.9335	.9336	.9335	.9334	.9334	.9347	.9335	.9335	.9335
Threshold	225	218	218	230	216	218	211	225	227	218	216	216	233	218	222	225
Sensitivity	.0665	.0666	.0666	.0663	.0666	.0666	.0666	.0665	.0664	.0666	.0666	.0666	.0659	.0666	.0665	.0665
Specificity	.9773	.9969	.9846	.9414	.9958	.9863	.9950	.9969	.9871	.9890	.9984	.9978	.9658	.9889	.9941	.9913
ARoC	.2558	.3537	.2777	.2468	.3465	.3186	.3584	.3639	.3235	.3214	.3344	.3612	.2984	.2444	.2992	.2969
Accuracy	.9519	.9617	.9556	.9338	.9612	.9564	.9608	.9617	.9568	.9578	.9625	.9622	.9459	.9577	.9603	.9589
PPV	.7453	.9554	.8122	.5307	.9403	.8289	.9305	.9558	.8375	.8582	.9762	.9687	.6586	.8567	.9181	.8842
NPV	.5115	.5164	.5133	.5020	.5162	.5138	.5160	.5164	.5139	.5145	.5168	.5167	.5084	.5144	.5157	.5150
FNR	.9335	.9334	.9334	.9337	.9334	.9334	.9334	.9335	.9336	.9334	.9334	.9334	.9341	.9334	.9335	.9335
FPR	.0227	.6031	.0154	.0586	.0042	.0137	.0050	.0031	.0129	.0110	.0016	.0022	.0342	.0111	.0059	.0087
FDR	.2547	.0446	.1878	.4693	.0597	.1711	.0695	.0442	.1625	.1418	.0238	.0313	.3414	.1433	.0819	.1158
FOR	.4885	.4836	.4867	.4980	.4838	.4862	.4840	.4836	.4861	.4855	.4832	.4833	.4916	.4856	.4843	.4850
F1Score	.1221	.1245	.1231	.1178	.1244	.1233	.1243	.1244	.1231	.1236	.1247	.1247	.1199	.1236	.1241	.1237
MCC	.1060	.1731	.1291	.0159	.1688	.1346	.1659	.1731	.1372	.1439	.1790	.1769	.0728	.1435	.1621	.1519
MK	.2568	.4718	.3255	.0328	.4565	.3427	.4465	.4722	.3514	.3727	.4930	.4854	.1670	.3711	.4338	.3992

Segmentation is properly conducted, can mend the level of accuracy for detecting and characterizing lesions. The research paper focused on the anticipated techniques for accomplishing the job of segmenting the mammogram images with enhanced readings of the evaluated performance parameters. The adopted technique performed reasonably well and would prove useful for conducting the appropriate classification of the mammogram images.

***Conflict of Interest - On behalf of all authors, the corresponding author states that there is no conflict of interest.**

REFERENCES

[1]. N. Saidin, H.A.M. Sakim, U.K. Ngah, I.L. Shuaib, "Segmentation of breast regions in mammogram based on density: a review", International Journal of Computer Science Issues, Vol. 9, No. 4, pp. 108–116, 2012.

[2]. B. Zheng, J.H. Sumkin, M.L. Zuley, X. Wang, A.H. Klym D. Gur, "Bilateral mammographic density asymmetry and breast cancer risk: a preliminary assessment", European Journal of Radiology, Vol. 80, No. 11, pp. 3222–3228, 2012.

[3]. F. Khalvati, C. Gallego-Ortiz, S. Balasingham, A.L. Martel, "Automated segmentation of breast in 3-D MR images using a robust atlas", IEEE Transactions on Medical Imaging, Vol 34, pp. 116–125, 2015.

[4]. A. Gubern-Merida, M. Kallenberg, R.M. Mann, R. Marti, N. Karssemeijer, "Breast segmentation and density estimation in breast mri: a fully automatic framework", IEEE Journal of Biomedical and Health Informatics, Vol. 19, No. 1, pp. 349–357, 2015.

[5]. R. Llobet, M. Pollan, J. Anton, "Semi-automated and fully automated mammographic density measurement and breast cancer risk prediction", Computer Methods and Programs in Biomedicine, Vol. 116, No. 2, pp. 105–115, 2014.

[6]. M. Mustra, M. Grgic, R.M. Rangayyan, "Review of recent advances in segmentation of the breast boundary and the pectoral muscle in mammograms", Medical & biological engineering & computing, Vol. 54, No. 7, pp. 1–22, 2015.

[7]. K. He, X. Zhang, S. Ren, J. Sun, "Delving deep into rectifiers: surpassing human-level performance on IMAGENET classification", in Proceedings of the IEEE International Conference on Computer Vision., pp. 1026 – 1034, IEEE, 2015.

[8]. M.L. Giger, N. Karssemeijer, J.A. Schnabel, "Breast image analysis for risk assessment, detection, diagnosis, and treatment of cancer", Annual Review of Biomedical Engineering, Vol. 15, pp. 327 –357, 2013.

[9]. I.C. Moreira, "INbreast: toward a full-field digital mammographic database", Academic Radiology, Vol. 19, No. 2, pp. 236 –48, 2012.

[10]. E.Kozegar, M.Soryani, B.Minaei, I.Domingues, "Assessment of a novel mass detection algorithm in mammograms", Journal of Cancer Research and Therapeutics, Vol. 9, No. 4, pp. 592 –600, 2013.

[11]. N. Dhungel, G. Carneiro, A.P. Bradley, "A deep learning approach for the analysis of masses in mammograms with minimal user intervention", Medical Image Analysis, Vol. 37, pp. 114 –128, 2017.

[12]. A. Becker, "Deep learning in mammography: diagnostic accuracy of a multipurpose image analysis software in the detection of breast cancer", Investigative Radiology, Vol. 52, pp. 434 –440, 2017.

[13]. S. Ghosh, G. Samanta, M.D.L. Sen, "Multi-Model Approach and Fuzzy Clustering for Mammogram Tumor to Improve Accuracy", Computation, MDPI, Vol. 9, No. 59, pp. 1 – 15, 2021.

[14]. N. Saffari, H.A. Rashwan, M. Abdel-Nasser, V. K. Singh, M. Arenas, E. Mangina, B. Herrera, D. Puig, "Fully Automated Breast Density Segmentation and Classification Using Deep Learning", Diagnostics, MDPI, Vol. 10, No. 988, pp. 1 – 20, 2020.

[15]. N. Alam, E.R.E. Denton, R. Zwiggelaar, "Classification of Microcalcification Cluster in Digital Mammograms Using a Stack Generalization Based Classifier", MDPI, Journal of Imaging, Vol. 2019, pp. 1 – 24, 2019.

[16]. M.Y. Kamil, M. Salih, "Breast Tumor Detection via Fuzzy Morphological Operations", International Journal of Advanced Pervasive and Ubiquitous Computing, Vol. 11, pp. 33-44, 2019.

[17]. A.A. Delphia, M. Kamarasan, S. Sathiamoorthy, "Image Processing For Identification of Breast Cancer: A Literature Survey", Asian Journal of Electrical Sciences, Vol. 7, No. 2, pp. 28-37, 2018.

[18]. D. Pandeya, X. Yinb, H. Wanga, M.Y. Suc, J.H. Chen, J. Wu, Y. Zhang, "Automatic and fast segmentation of breast region-of-interest (ROI) and density in MRIs", Elsevier, Heliyob, Vol. 2018, pp. 1 – 30, 2018.

[19]. K.D. Marcomini, D. Karem, A.A.O. Carneiro, H. Schnabel, "Application of artificial neural network models in segmentation and classification of nodules in breast ultrasound digital images", International Journal of Biomedical Imaging, Vol. 2016, pp. 1-13, 2016.

AUTHOR PROFILES

Sarbjit Kaur is pursuing a Ph.D. in Image processing from RIMT University, Mandi Gobindgarh, Punjab. She has completed her M.Phil.(CS) from Chaudhary Devi Lal University, Sirsa. She obtained her MCA degree from Maharishi Dayanand University, Rohtak with distinction. She is having more than 17 years of Teaching Experience. She has published more than 16 research papers in National, International Journals and Conferences.

Dr. Jasmeen Gill is presently serving as Associate Professor Department of Computer Science and Engineering, RIMT University, Mandi Gobindgarh, India. He has about 15 years of experience in teaching and research. She has guided five Ph.D. research scholars and four others are under her supervision. She has published 30 research papers in International and Indian Journals and Conferences.

Dr. Gagandeep Jagdev is currently serving as a faculty member at the Dept. of Computer Science, Punjabi University Campus GKC, Damdama Sahib (PB). His total teaching and research experience is more than 14 years and has 152 International and National publications in reputed journals and conferences to his credit. He is also a member of the editorial board of several reputed International Journals indexed in ESCI, Scopus, ACM, WoS, and Pubmeds and has been an active Technical Program Committee member of several International and National conferences conducted by renowned universities and academic institutions. He has been bestowed with Best Research Paper awards 3 times by the Government College of Engineering and Technology, Jammu in 2015 and 2021 and by NITTTR, Chandigarh at ICCCN – 2017. His field of expertise is Big Data Analytics, Data Science, Image processing, Cloud Computing, Cloud Security, Cryptography, and WANETs.